



Bromide counterion as a spectroscopic sensor at the interface of cetyltrimethylammonium micelles

Melisa Hermet, Laura Bakás, Susana R. Morcelle, Delia L. Bernik *

Plant Proteins Research Center (CIProVe), National University of La Plata, Calles 47 y 115, CP1900, La Plata, Buenos Aires, Argentina

ARTICLE INFO

Article history:

Received 12 February 2019
Received in revised form 31 May 2019
Accepted 9 June 2019
Available online 24 June 2019

Keywords:

Bromide absorption
UV spectra
Cetyltrimethylammoniumbromide
Micelles
Pyrene excimer
Interface
CTAB

ABSTRACT

The strong UV absorption of the bromide in aqueous solution undergoes a remarkable red shift of more than 10 nm induced by the addition of the salts that constitute a saline buffer. The maximum absorption wavelength of the bromide is displaced from approximately 194 nm in ultrapure water to wavelengths above 200 nm, depending on the composition of the solution. The bromide spectrum as counterion of the cetyltrimethylammonium in the surfactant CTAB also shows sensitivity to the aggregation behavior of the tensioactive, being able to detect intermolecular interactions even at concentrations lower than the critical micelle concentration. And, when the micelles are assembled, the bromide absorption detects the interfacial rearrangements caused by the incorporation of ions. To know more about those interfacial features, the pyrene molecular probe was used, taking advantage of the extensive knowledge of its spectroscopy. Pyrene verifies the existence of changes in the interfacial organization which confirm that the sensitivity of the bromide spectrum is based on the ability of the ion to detect its microenvironment, and therefore reaffirms that its absorption spectrum can be used as a local sensor. The present work encourages the use of bromide as a sensor ion in the UV region between 190 and 210 nm, which would avoid the introduction of external molecular probes that could disturb the system.

© 2019 Elsevier B.V. All rights reserved.

1. Introduction

Interfaces in biological systems are the gateway for molecules and ions, an unavoidable path for communication. The use of model systems of interfaces and their study by means of molecular probes always offers new information that is worth analyzing to build the puzzle, the global picture. As simple models, micelles are a preferred study system, since parameters such as composition, charge, size, among others, can be widely and simply modulated.

For structural studies it would be ideal to have a spectroscopic sensor not foreign to the system, to gather information without altering the molecular organization by introducing a probe. Here we show that bromide can be that sought constituent. This halide, a regular counterion of several tensioactives, has already shown to have particular characteristics from the structural point of view, imparting concrete adsorption and aggregation properties [1,2]. The absorption spectra of undissociated molecules of alkali halides have been determined in the vapor phase, where the bromide shows a strong absorption band near 200 nm [3]. More recently, the absorption of calcium bromide was suggested as analytical methodology for the determination of bromide in samples [4,5].

The results reported here show another aspect that takes advantage of the strong UV absorption of the bromide ions in aqueous solutions. Using simple spectrophotometers the remarkable changes in the bromide absorption spectrum can be used to study the relationship of the halide ion with its counterion and other molecules in solution. In many cases these absorption of bromide in solution have been ignored or disregarded. This could have been because the wavelengths of bromide absorption in ultrapure water, centered at about 193 nm, are far from the range of absorption of many chromophoric groups. This work shows that, depending on the solution composition, bromide absorption can displace at 205 nm or even to longer wavelengths, and with a high molar absorptivity. Moreover, in particular cases where bromide is the counterion of molecules experiencing self-aggregation, such as surfactants, the changes in its absorption spectrum acts as a sensor of aggregation and interaction with other ions or molecules bound or inserted at the interfacial region, interactively detecting its microenvironment.

With this purpose we use CTAB, cetyltrimethylammonium bromide, to find out about the sensitivity of the bromide spectra. CTAB is, in turn, representative of the quaternary ammonium surfactants, known as QAS, an extensive family of cationic tensioactives with wide application in fields such as gene transfection, in analytical separation techniques, and as antimicrobial agents [6–8]. Whatever the process faced by a QAS surfactant, the action involves unarguably an interaction at the

* Corresponding author.
E-mail address: dbernik@biol.unlp.edu.ar (D.L. Bernik).

interface level with a leading role of the quaternary ammonium, where the counterion also plays a significant part in the overall process. As a witness to these phenomena, the pyrene (Py) molecular probe was used, taking advantage of the extensive knowledge of its spectroscopy. Throughout the work we present the parallel results obtained with both molecules in order to better interpret the changes observed.

2. Experimental

2.1. Chemicals

Hexadecyltrimethylammonium bromide was purchased from Ciccarelli. Pyrene (Py) was provided by Sigma-Aldrich (99.0% pure). Ultrapure water was MilliQ® grade. All the other reagents were of analytical grade.

2.2. Sample preparation

CTAB solutions were prepared by weighing the appropriate amount of surfactant and dissolving it in the corresponding water solution with gentle mixing. Pyrene stock solution was prepared by dissolving a small amount of solid in ethanol checking its concentration by absorbance using the molar absorption coefficient (ϵ) $54,000 \text{ M}^{-1} \text{ cm}^{-1}$ at 335 nm [9]. Small aliquots of this concentrated stock were added to the surfactants samples just prior to the absorbance and fluorescence measurements in a way that the ethanol final ratio to water was always below 1% v/v. All surfactant solutions and samples were prepared in plastic (PP) volumetric materials in order to diminish both pyrene and surfactant adsorption to the glass walls. PBS was prepared such that the osmolarity results isotonic with biological material (300 mOsm/L); 123.3 mM NaCl, 22.2 mM Na_2HPO_4 , 5.6 mM KH_2PO_4 in ultrapure water (milliQ®), final pH 7.4 [10].

2.3. Absorbance and fluorescence measurements

Absorbance spectra were recorded with an Agilent 8453 and PGT60 spectrophotometers, using quartz and suprasil cuvettes with a path length of 1 cm. A Shimadzu RF1501 spectrofluorometer was used to record the pyrene fluorescence spectra, with excitation and emission fluorescence slits of 10 nm. The excitation wavelength was 335 nm and the emission wavelengths are indicated in the legends of the Figures. All the experiments were carried out at 22–25 °C.

3. Results and discussion

3.1. Bromide counterion and pyrene: two probes for the polar head region in micelles

Fig. 1a) shows the drastic change of bromide (CTAB) absorption spectra when changing from ultrapure deionized water to a biologically

isoosmotic saline buffer (PBS), reflected in a ten nanometers shift with a sharp reduction of bandwidth.

Simultaneously, the part b) in the Figure shows how the fluorescent probe Py senses the change at the interface: the black curve is the fluorescence spectrum when pyrene is associated to CTAB incipient micelles in pure water, CTAB- H_2O , whereas the blue curve is the one obtained in phosphate buffer saline, CTAB-PBS. Determination of the CMC in each media is detailed in the Supplementary material.

Impelled by these contrasts, we first studied changes in the absorption spectrum of bromide (i.e. CTAB) in different media. A parallel analysis of the information provided by the pyrene molecular probe allows us to propose an explanation of the structural changes that give rise to these remarkable differences. Being bromide herein the counterion of a surfactant molecule, we must also analyze the system below and above the critical micelle concentration of CTAB in the respective solutions.

3.2. Bromide counterion as sensor of other ions in solution

The strong absorption of halide ions in the far UV has been described earlier [11–13]. As a surfactant with bromide as counterion, the spectrum of a CTAB solution in ultrapure water gives a broad band centered at about 193–194 nm (Fig. 1a, black curve). The broadness of the band is due to an unresolved splitting of the bromide absorption, being the wavelengths of each component 191 ± 1 and 198 ± 2 nm [14,15].

The spectra shown in Fig. 1 were recorded in two media with differences in pH and in the content of salts. First it is necessary to find out if the pH difference between the one of water and that of PBS (7.4) influences the spectra. The pH of pure water is around 6, depending on temperature and pressure, due to dissolved carbon dioxide and its corresponding hydration and dissociation equilibrium [16]. We verified that the absorption spectrum of CTAB obtained in pure water and in 1.5 mM phosphate buffer pH 7.4 remained invariant. Hence, we tested the absorption of CTAB in aqueous solutions at increasing concentrations of sodium chloride (Fig. 2), since this salt is the most abundant component of the PBS buffer.

The spectra show a pronounced bathochromic shift of about ten nanometers and, in addition, a significant decrease in absorbance with the increase in salt concentration. At concentrations in the range of 10^{-5} M in PBS, that is, well below the CMC, CTAB spectra show a linear relationship between the maximum absorption value and the concentration. This allows calculating the molar absorption coefficient to be $5.65 \cdot 10^3 \text{ M}^{-1} \text{ cm}^{-1}$ at 202.5 nm (the maximum absorption wavelength at those surfactant concentrations). This is almost half the absorption coefficient previously reported for CTAB in ultrapure water at 194 nm ($\approx 1.15 \cdot 10^4 \text{ M}^{-1} \text{ cm}^{-1}$) [14].

In the inset the spectra are shown normalized in order to compare with the spectra of CTAB in water and PBS previously shown in Fig. 1a; the similarity with that obtained in a 0.12 M NaCl solution

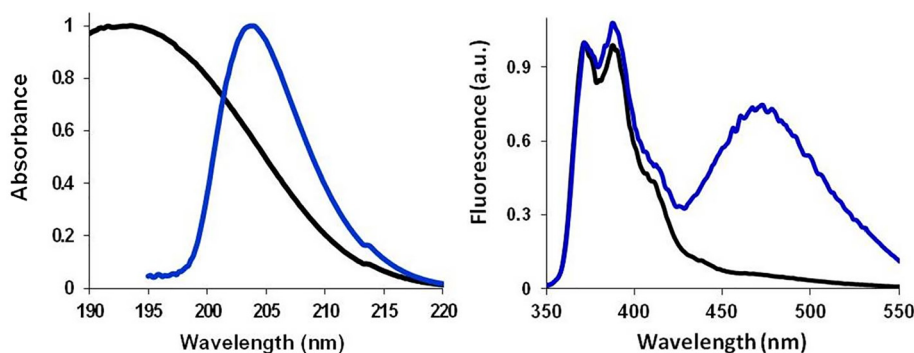


Fig. 1. a) Absorption spectra of bromide and b) fluorescence emission spectra of Py, in CTAB- H_2O (black curve) and CTAB-PBS (blue curve), at their respective CMC concentrations in each media (0.9 mM in ultrapure water and 0.5 mM in PBS).

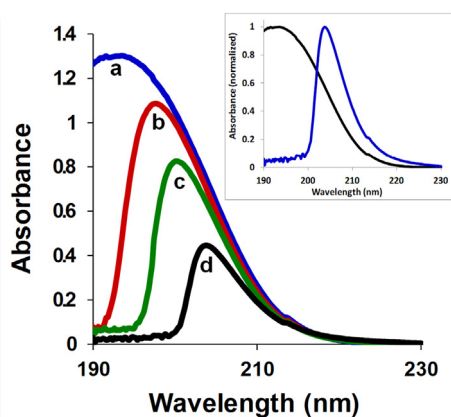


Fig. 2. Absorption spectra of a CTAB solution in: a-in ultrapure water (0.12 mM, upper curve), and after successive additions of aliquots of a NaCl solution to get in b, c and d NaCl concentrations of 0.052, 0.09 and 0.12 M, respectively. Inset: the spectra in pure water and in 0.12 M NaCl solution are normalized to show the similarity with the spectra in Fig. 1a.

suggests that the sodium chloride content in the PBS is the main source of the change.

It has been proposed that the sensitivity of the halide spectra originates in the influence of the dipole layers of the solvent molecules oriented around the ion. For example, in the case of iodide, previous studies showed that the low frequency peak of the first electronic absorption band changes markedly when the solvent or the temperature change. However, the absorption spectra of iodide do not change with the addition of sodium chloride, unlike the noticeable changes we obtained here with bromide [17].

3.3. Bromide as a sensor of aggregation

The sensitivity of the bromide to its microenvironment is not limited to the presence of salts in the solution. Even leaving the medium invariant, we observed changes in CTAB spectra simply by increasing its concentration, at a constant temperature. First, the CMC of CTAB in PBS was found to be 0.5 mM, using the Py fluorescent probe by a procedure detailed in the Supplementary material. Fig. 3 depicts the evolution of bromide absorption spectra in PBS at increasing CTAB concentrations. The progressive shift to wavelengths above 203 nm is noticeable; however,

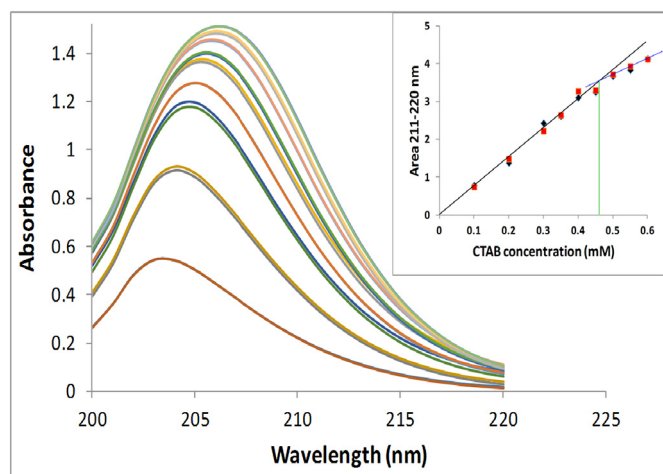


Fig. 3. Absorbance spectra of CTAB in PBS. From bottom to top CTAB concentrations are: 0.1, 0.2, 0.3, 0.35, 0.4, 0.45, 0.5, 0.55 and 0.6 mM. The curves are shown in duplicate of different samples, to highlight the reproducibility. Inset: plot of the area under the curves between 210 and 230 nm, (region where the absorbance is less than 1) vs CTAB concentration. The two straight lines intercept at a value of 0.46 mM of CTAB.

given the high absorptivity, the exact values at the maxima of absorbance should be confirmed with shorter optical paths.

By integrating the area under the curve of each spectrum between 210 and 230 nm (a region where the absorbance is less than 1) we can construct the graph displayed in the inset. The plot of the areas as a function of CTAB concentration shows a change in the slope at about 0.46 mM CTAB, estimated from the intersection of two straight lines. This value is very similar to that found by means of Py fluorescence. Therefore, Fig. 3 is convincing evidence that the bromide absorption spectra are capable of detecting the aggregation of CTAB molecules to form micelles. Later in Section 3.6 we will return to this topic with additional studies in this regard.

3.4. Parallel spectroscopic studies with pyrene at the CTAB interface

Given the vast knowledge of pyrene spectroscopy, this molecular probe was used under conditions equivalent to those studied with bromide, in order to elucidate the structural features that give rise to the observed spectroscopic changes.

Fig. 1b shows that the fluorescent probe pyrene, when interacting with CTAB, also evidences a striking difference between the spectra displayed in pure water and in PBS. Given that Py interacts at the interface level, its absorption and fluorescence spectra were analyzed in similar conditions to those assayed with bromide, to gain more information on the system.

One distinctive characteristic of Py, an electron-rich polyaromatic hydrocarbon, is its excimer fluorescence in the cyano-green region of the spectrum (470–500 nm), which has been documented to be maximum at the CMC of a surfactant [18,19]. Indeed, the excimer signal at 480 nm is prominent at the CMC in CTAB-PBS samples, whereas it can hardly be observed in CTAB-H₂O. Taking into account that the excimer formation is directly related to the number of probe molecules in the micelle (called occupation number, N_{occ}), the assay was repeated for a wide range of Py concentrations, as shown in the Fig. 4.

From the spectra of Fig. 4, the characteristic I₃/I₁ ratio for the analysis of the information given by the Py is calculated as described in the Supplementary material. Also, the absorption spectra of same samples were analyzed simultaneously, to obtain as much information as possible; the results are shown in Fig. 5. The values of I₃/I₁ proved to be independent of the concentration of Py, either in PBS or in water and for concentrations of CTAB below, at or above the CMC in both media.

Below the CMC the I₃/I₁ ratio has the same value both in CTAB-H₂O and CTAB-PBS. Along increasing CTAB concentration in pure water the I₃/I₁ increases in total only 2%, whereas in CTAB-PBS the changes are noticeable, with increases of 10% and 23% at and above the CMC, respectively, in comparison with the average value obtained below the CMC. Hence, the magnitude of the change in the I₃/I₁ ratio is another noticeable difference between CTAB-H₂O and CTAB-PBS.

The absorption spectra of the samples whose fluorescence spectra are shown in Fig. 4 were recorded and analyzed. Some aspects worth to be highlighted are plotted in Fig. 5b. The absorption of Py in CTAB-PBS is much higher than in CTAB-H₂O at and above the CMC, as shown in the graph of absorption maxima versus the concentration of Py. The maximum absorption wavelength, initially at 335 nm below CMC in both media, remains unchanged in CTAB-H₂O but shifts to 337–338 nm in CTAB-PBS at and above the CMC. The invariance of Py spectra for concentrations at and above the CMC in CTAB-H₂O is remarkable, and appears to come from samples in the absence of micelles. The inset highlights the differences of pyrene absorption bands in CTAB-H₂O and CTAB-PBS above the CMC. The information given by these studies suggest, taking also into account the previously described I₃/I₁ ratios, that Py remains in the outermost region of the interface in the samples of CTAB-H₂O, without being able to enter the region of the palisade, experiencing a greater aggregation due to its restricted location.

A more extensive and detailed analysis is developed in the Supplementary material.

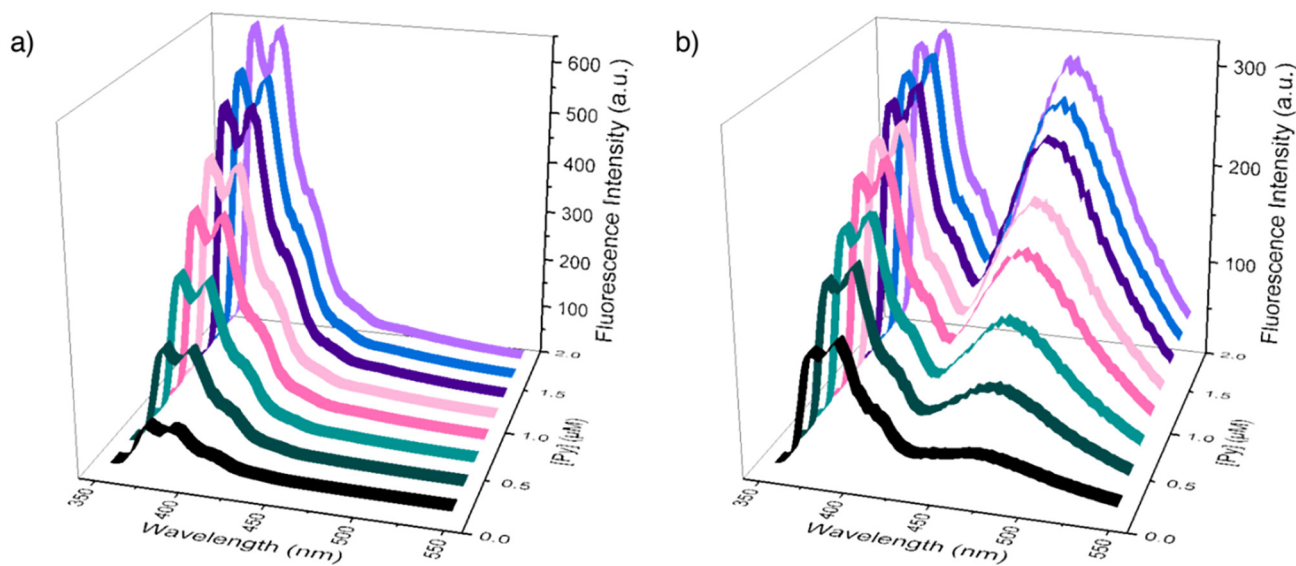


Fig. 4. Fluorescence emission spectra of increasing Py concentrations from 0.24 to 1.96 μM in a) CTAB-H₂O and b) CTAB-PBS at their respective CMC concentrations in each media (0.9 mM in water and 0.5 mM in PBS).

3.5. Relationship between bromide and pyrene spectra

In CTAB solutions in the absence of salts an intimate interaction between bromide and CTA⁺ is likely. According to preceding studies, some extent of ionic association as a solvent-shared ion pairs can be expected in pure water [20,21]. The addition of salt would weaken this ion-association and, by modifying the solvation layer of bromide, induces the shift from the broadband centered at 194 nm to a narrower band above 200 nm.

The formation of micelles undoubtedly generates an additional change in the microenvironment of the bromide. Some bromides may remain closely associated with their CTA⁺ counterion, but given the steric hindrance, there must be a redistribution of bromides between the Stern and diffuse layers. This would induce the changes in the absorption which allows the determination of the CMC by integrating the area under the spectra through the transition.

This analysis about the origin of the observed changes in bromide spectra is coherent with the information given by the molecular probe pyrene. It has been reported that the electron-deficient cetyltrimethylammonium ion (CTA⁺) selectively deactivates the

fluorescence of the Py excimer by dynamic quenching [22]. This quenching was early mentioned by Almgren et al. and Lianos et al., who found that quaternary ammonium compounds interact with a certain affinity with Py, inhibiting the fluorescence of its excimer [20,21]. Moreover, in the particular case of CTAB in water, it was proposed that CTA⁺ and pyrene form a weak complex, to which bromide is attached, forming an ion-pair [23]. A sign of this close CTA⁺-Py interaction in pure water is the almost invariant I₃/I₁ ratio in CTAB-H₂O shown in Fig. 2. Recently, studies with other QAS also reported similar trends of anomalous I₃/I₁ ratios [24].

The change in the interfacial arrangement introduced by the PBS is what the scheme in Fig. 6 is intended to describe: when introducing the buffer salts, the bromide counterions and the pyrene are partially released from their close association with CTA⁺. The bromide redistributes (the binding changes), the pyrene moves to a less polar microenvironment in the palisade region, and the excimer recovers fluorescence intensity.

Another test supporting the interpretation of pyrene excimer dequenching by the addition of salts is described in the Supplementary material.

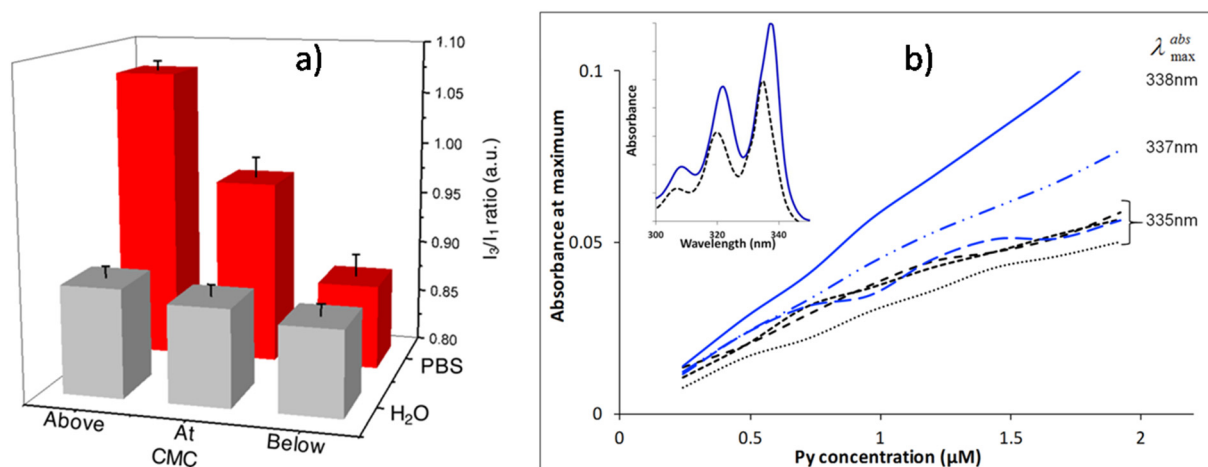


Fig. 5. a) Comparison of the I₃/I₁ ratios of Py in CTAB-H₂O and CTAB-PBS samples for surfactant concentrations below, at and above the CMC in each medium. Ratios are expressed as the mean \pm SD of the eight Py concentrations assayed for each surfactant concentration. b) Graphs of the absorption at the maximum absorption wavelength as a function of Py concentrations of same samples. Inset: comparison of the lowest energy band of the absorption spectra of pyrene in CTAB-H₂O (black dashed line) and in CTAB-PBS (blue full line).

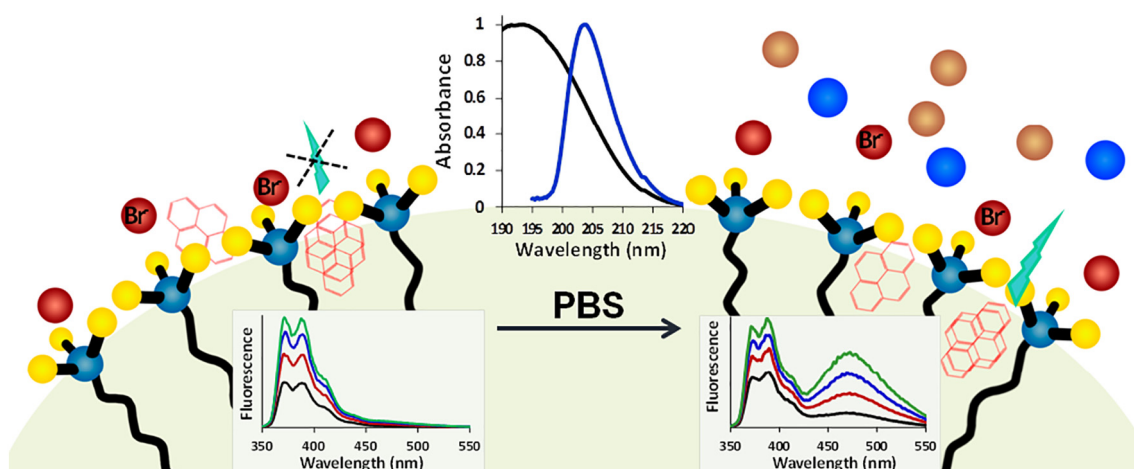


Fig. 6. Scheme of the interfacial arrangement of the polar head region of the CTAB and its bromide counterion before and after the addition of the buffer. The red spheres represent Br^- , blue Na^+ , brown Cl^- . Above, in the center, the bromide absorption spectra in pure water (black line) and in PBS (blue line) are shown. Below, the fluorescence spectra of different concentrations of pyrene in CTAB at the CMC in pure water (left) and in PBS (right), and the proposed location of pyrene in each medium is drawn. In water, Py remains in the outer region of the interface, while relocates in the region of the palisade after the addition of buffer.

3.6. Additional information given by bromide absorption spectra

Regarding the change in the bromide spectra observed for increasing concentrations of CTAB in PBS (see Fig. 3), it is worth drawing attention to the information given by these bathochromic shifts. Well below the CMC the spectrum is centered at about 202 nm and progressively moves above 205 nm as the concentration approaches and exceeds the value of the CMC. Given the high bromide absorbance in PBS, we alternatively studied CTAB's CMC in more concentrated saline solutions (NaCl 0.5 and 1 M). As previously shown in Fig. 2, increasing salt concentrations significantly decrease the absorbance, thus allowing the analysis of the spectral shifts in more detail.

Fig. 7 shows the progressive shift of CTAB absorption spectra in a 0.5 M NaCl solution. The plot of the spectral areas vs CTAB concentrations tracks down the CMC at around 0.13 mM. An analogous procedure but in a 1 M NaCl solution locates the CMC at CTAB 0.04 mM.

The inset shows how evolves the value of the maximum absorption wavelength ($\lambda_{\text{max}}^{\text{Abs}}$) during the monomer-micelle transition. Both for the

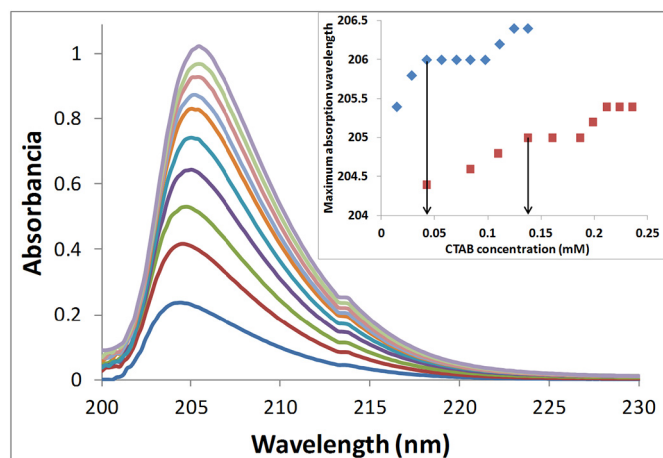


Fig. 7. Absorption spectra of CTAB increasing concentrations in aqueous 0.5 M NaCl solution. Increasing CTAB concentrations in NaCl 0.5 M are: 0.043, 0.082, 0.135, 0.16, 0.186, 0.198, 0.211, 0.223 and 0.235. Inset: graph of the maximum absorption wavelength ($\lambda_{\text{max}}^{\text{Abs}}$) as a function of CTAB concentration in NaCl solutions 0.5 M (red squares) and 1 M (blue diamonds). The arrows points the CTAB CMC determined in each medium

CTAB in 0.5 M NaCl solution and for the 1 M solution of the salt, the $\lambda_{\text{max}}^{\text{Abs}}$ shifts to the red with increasing surfactant concentration, remaining invariant in a narrow range before returning to move further to the red. The onset of that first plateau coincides in both cases with the value of the CMC in the respective media. The pattern observed for CTAB in PBS is similar.

Our interpretation is that the sensitivity of bromide absorption is such that the spectrum begins to detect other surfactant molecules even below the CMC, which is not unexpected given the high concentration of salt, which can promote that the long hydrocarbon chains of the CTAB aggregate at a certain pre-CMC concentration. Once the micelles began to assemble, the microenvironment of the bromide remains invariant until a given additional increase in the concentration of CTAB affects the packing of surfactant in the micelle, which alters the interaction of the bromide with neighboring molecules and probably also its degree of binding to its CTA^+ counterion. This is an additional aspect of the bromide spectrum to be exploited in different situations.

3.7. Perspectives

A wide range of applications arises from the high sensitivity of the absorption spectrum of bromide. The studies may be extended to other surfactants or biomolecules containing bromide as counterion. Given the high absorptivity of the bromide, its spectra can be detected well at very low concentrations; therefore it can sense aggregation phenomena at the micromolar level. The binding of bromide as a counterion could be sensitive to the insertion of foreign molecules in its microenvironment or to the changes induced by chemical reactions, either in a micelle or in other biologically relevant interfaces.

4. Conclusions

The remarkable sensitivity to the absorption spectra of bromide in aqueous is shown here for the first time. Spectral shifts that can reach 10–15 nm can be achieved at different concentrations and solution compositions; the microenvironment also modifies the molar extinction coefficient. The spectra can, in addition, be affected by aggregation processes of the molecules carrying bromide as counterion. These properties can be largely exploited in future research both in homogeneous and heterogeneous systems.

Acknowledgements

MH is recipient of a doctoral fellowship of CONICET. LB belongs to the CICIPBA researcher career. DLB and SRM belong to the CONICET researcher career. Financial support of MINCYT (PICT 2013-00647) and UNLP (X11-682 and X11-828) are acknowledged.

Appendix A. Supplementary data

Supplementary data to this article can be found online at <https://doi.org/10.1016/j.saa.2019.117266>.

References

- [1] M. In, V. Bec, O. Aguerre-Chariol, R. Zana, Quaternary ammonium bromide surfactant oligomers in aqueous solution: self-association and microstructure, *Langmuir* 16 (2000) 141–148, <https://doi.org/10.1021/la990645g>.
- [2] J.P. Vivek, I.J. Burgess, Quaternary ammonium bromide surfactant adsorption on low index surfaces of gold. 2. Au(100) and the role of crystallographic dependent adsorption in the formation of anisotropic nanoparticles, *Langmuir* 28 (2012) 5040–5047, <https://doi.org/10.1021/la300036y>.
- [3] G. Daminelli, D.A. Katskov, R.M. Mofolo, P. Tittarelli, Atomic and molecular spectra of vapours evolved in a graphite furnace. Part 1. Alkali halides, *Spectrochim. Acta B* 54 (1999) 669–682, [https://doi.org/10.1016/S0584-8547\(98\)00248-1](https://doi.org/10.1016/S0584-8547(98)00248-1).
- [4] M.R. Flórez, M. Resano, Direct determination of bromine in plastic materials by means of solid sampling high-resolution continuum source graphite furnace molecular absorption spectrometry, *Spectrochim. Acta B* 88 (2013) 32–39, <https://doi.org/10.1016/j.sab.2013.07.013>.
- [5] E.R. Pereira, I.N.B. Castilho, B. Welz, J.S. Gois, D.L.G. Borges, E. Carasek, J.B. de Andrade, Method development for the determination of bromine in coal using high-resolution continuum source graphite furnace molecular absorption spectrometry and direct solid sample analysis, *Spectrochim. Acta B* 96 (2014) 33–39, <https://doi.org/10.1016/j.sab.2014.04.001>.
- [6] P. Gilbert, L.E. Moore, Cationic antiseptics: diversity of action under a common epithet, *J. Appl. Microbiol.* 99 (2005) 703–715, <https://doi.org/10.1111/j.1365-2672.2005.02664.x>.
- [7] Z.H. Asadov, G.A. Ahmadova, R.A. Rahimov, A.Z. Abilova, S.H. Zargarova, F.I. Zubkov, Synthesis and properties of quaternary ammonium surfactants based on alkylamine, propylene oxide, and 2-chloroethanol, *J. Surfactant Deterg.* 21 (2018) 247–254, <https://doi.org/10.1002/jsde.12008>.
- [8] E. Fuguet, C.M. Rafols, M. Roses, E. Bosch, Critical micelle concentration of surfactants in aqueous buffered and unbuffered systems, *Anal. Chim. Acta* 548 (2005) 95–100, <https://doi.org/10.1016/j.aca.2005.05.069>.
- [9] I.B. Beriman, *Handbook of Fluorescence Spectra of Aromatic Molecules*, Academic Press, New York, 1971.
- [10] M.E. Fait, M. Hermet, F. Comelles, P. Clapes, H.A. Alvarez, E. Prieto, V. Herlax, S.R. Morcelle, L. Bakas, Microvesicle release and micellar attack as the alternative mechanisms involved in the red-blood cell-membrane solubilization induced by arginine based surfactants, *RSC Adv.* 7 (2017) 37549–37558, <https://doi.org/10.1039/C7RA03640J>.
- [11] O. Zielinski, D. Voß, B. Saworski, B. Fiedler, A. Körtzinger, Computation of nitrate concentrations in turbid coastal waters using an in situ ultraviolet spectrophotometer, *J. Sea Res.* 65 (2011) 456–460, <https://doi.org/10.1016/j.seares.2011.04.002>.
- [12] E.A. Guenther, K.S. Johnson, K.H. Coale, Direct ultraviolet spectrophotometric determination of total sulfide and iodide in natural waters, *Anal. Chem.* 73 (2001) 3481–3487, <https://doi.org/10.1021/ac0013812>.
- [13] J. Mertens, D.L. Massart, Determination of nitrate ion in marine biotopes with high nitrate content by ultraviolet spectrophotometry, *Bull. Soc. Chim. Belg.* 80 (1971) 151–158, <https://doi.org/10.1002/bscb.19710800116>.
- [14] T.G. Movchan, E.V. Plotnikova, O.G. Us'yarov, Light absorption in solutions of cetyltrimethylammonium and cetylpyridinium bromides, *Colloid J.* 75 (2013) 319–325, <https://doi.org/10.1134/S1061933X13030137>.
- [15] J. Jortner, A. Treinin, Intensities of the absorption bands of halides ions in solution, *Trans. Faraday Soc.* 58 (1962) 1503–1510, <https://doi.org/10.1039/TF9625801503>.
- [16] Z. Duan, R.S. Sun, An improved model calculating CO₂ solubility in pure water and aqueous NaCl solutions from 273 to 533 K and from 0 to 2000 bar, *Chem. Geol.* 193 (2003) 257–271, [https://doi.org/10.1016/S0009-2541\(02\)00263-2](https://doi.org/10.1016/S0009-2541(02)00263-2).
- [17] M. Smith, C.R. Symons, Solvation spectra. Part I. – the effect of environmental changes upon the ultra-violet absorption of solvated iodide ions, *Trans. Faraday Soc.* 54 (1958) 338–345, <https://doi.org/10.1039/TF9585400338>.
- [18] N.J. Turro, P. Kuo, Pyrene excimer formation in micelles of nonionic detergents and of water-soluble polymers, *Langmuir* 2 (1986) 438–442, <https://doi.org/10.1021/la00070a011>.
- [19] L. Piñeiro, M. Novo, W. Al-Soufi, Fluorescence emission of pyrene in surfactant solutions, *Adv. Colloid Interf. Sci.* 215 (2015) 1–12, <https://doi.org/10.1016/j.cis.2014.10.010>.
- [20] P. Lianos, M.L. Viriot, R. Zana, Study of the solubilization of aromatic hydrocarbons by aqueous micellar solutions, *J. Phys. Chem.* 88 (1984) 1098–1101, <https://doi.org/10.1021/j150650a014>.
- [21] M. Almgren, B. Medhage, E. Mulchtar, Fluorescence study of the weak interaction between pyrene and quaternary ammonium groups, *J. Photochem. Photobiol. A Chem.* 59 (1991) 323–334, [https://doi.org/10.1016/1010-6030\(91\)87084-9](https://doi.org/10.1016/1010-6030(91)87084-9).
- [22] K.S. Focsaneanu, J.C. Scaiano, Potential analytical applications of differential fluorescence quenching: pyrene monomer and excimer emissions as sensors for electron deficient molecules, *Photochem. Photobiol. Sci.* 4 (2005) 817–821, <https://doi.org/10.1039/b505249a>.
- [23] M. Almgren, F. Grieser, J.K. Thomas, Dynamic and static aspects of solubilization of neutral arenes in ionic micellar solutions, *J. Am. Chem. Soc.* 101 (1979) 279–291, <https://doi.org/10.1021/ja00496a001>.
- [24] H. Xing, P. Yanb, J. Xiao, Unusual location of the pyrene probe solubilized in the micellar solutions of tetraalkylammonium perfluorooctanoates, *Soft Matter* 9 (2013) 1164–1171, <https://doi.org/10.1021/j150650a014>.